Relationship Between Electrostatic Discharges on Spacecraft P78-2 and the Electron Environment

Harry C. Koons* and David J. Gorney†
The Aerospace Corporation, Los Angeles, California 90009

The relationship between the energetic electron environment and electrostatic discharges on the P78-2 (SCATHA) spacecraft has been examined. Internal discharges occur near perigee, whereas surface discharges occur uniformly over the radial range covered by SCATHA from 5.5 to 8 R_e. Surface discharges peak at local midnight and decrease toward local morning, whereas the internal discharges have a broad occurrence maximum centered on local noon. Both types are far more likely to occur when the Earth's magnetic field is disturbed. Although few surface discharges occur when the planetary magnetic index Kp is <4, a modest number of internal discharges occur under these quiet to normal conditions. Surface discharges have a strong tendency to occur when the flux of electrons with energies of tens of keV is high, whereas internal discharges occur when the flux of electrons with energies of hundreds of keV is high and the flux of tens of keV electrons is low. A significant correlation has been found between the occurrence of discharges on SCATHA and an estimate of the energetic electron fluence at geosynchronous orbit obtained from a neural network model of the relativistic electron flux at geosynchronous orbit. The incidence of internal discharges at predicted daily fluences above 10^{10} electrons/cm^2 is sufficiently high to warrant the use of this predictor to issue warnings for real-time satellite operations. The statistics of nine years of surface discharges on the SCATHA spacecraft are dominated by the single charging event on September 22, 1982.

Introduction

ELECTRONS in the space environment charge materials on the surface and inside a spacecraft. When the resulting electric field exceeds the breakdown field intensity for the material, an electrostatic discharge occurs. Electrostatic discharges are believed to have been responsible for a large number of spacecraft anomalies including command errors, phantom commands, degraded sensor performance, parts failure, and even complete loss of mission on a variety of spacecraft.[1-3]

DeForest[4] was the first to observe surface charging on a geosynchronous satellite. He found that ATS-5 charged to potentials as high as 10,000 V in eclipse and as high as 200 V in sunlight. He also noted that insulators near the aperture of his electron detector could be charged to several hundred volts without an accompanying change in the overall spacecraft potential. The first discharges aboard a satellite were reported by Shaw et al.[5] They detected discharges that occurred in the vicinity of transient sensors. The number of discharges increased during geomagnetically disturbed times and correlated with the anomalous behavior of subsystems on the spacecraft. Garrett[6] reviewed the theory and measurements of the charging of spacecraft surfaces.

Vampola[7] showed that the occurrence of anomalies onboard the U.S. Air Force Defense Support Program satellites coincided with significant increases in the flux of electrons >1.2 MeV as measured by the Geostationary Operational Environment Satellite (GOES) spacecraft and concluded that the anomalies were caused by thick dielectric charging. Thick dielectric charging or internal charging as we refer to it in this paper occurs when energetic electrons embed within dielectrics. This can build up electric fields inside a dielectric until its breakdown field intensity is reached.[8] Penetrating electrons can also charge well-insulated floating conductors below the surface of the vehicle.[9] Electromagnetic interference from the resulting electrostatic discharges is responsible for the anomalies.

In order to improve our understanding of the relationship between the environment and electrostatic discharges, we have examined the data from the P78-2 spacecraft charging at high altitudes (SCATHA) pulse analyzer, satellite surface potential monitors (SSPMs), energetic ion composition experiment, and the high energy particle spectrometer for a relationship between discharges and the electron environment. The SCATHA satellite was launched on January 30, 1979. The primary objective of the mission was to obtain environmental and engineering data that could be used for design guidelines and specifications to ensure that future spacecraft will operate satisfactorily in the plasma environment at synchronous orbit. The experiments are described by Stevens and Vampola[10] and Fennell.[11]

The engineering payloads include a pulse analyzer that measures the characteristics of electrical pulses in both the frequency and time domains. It measures the number of pulses, their amplitudes and their shapes with four sensors. It has been operating continuously since February 1979. Since that time, data from 1527 days have been analyzed. Pulses have been detected in response to spacecraft commands, during electron and ion beam operations, and during periods of natural surface charging. Previous papers have documented the occurrence of pulses during the first two years of the operation of the vehicle, their amplitudes, pulse shapes, and the correlation of these pulses with time periods when the surface samples on the vehicle are charged.[12-14]

Table 1 Distribution of pulses detected by the pulse analyzer in 1527 days of analyzed data

Type	Number
Command related	3158
s-tone cessation	2550
Beam experiments	2365
Natural discharges	316
Total	8389

Received Dec. 15, 1990; revision received May 15, 1991; accepted for publication May 21, 1991.

*Senior Scientist, Space Environment and Technology Center, P.O. Box 92957.

†Director, Atmospheric and Ionospheric Sciences Department, Space Environment and Technology Center, P.O. Box 92957. Member AIAA.

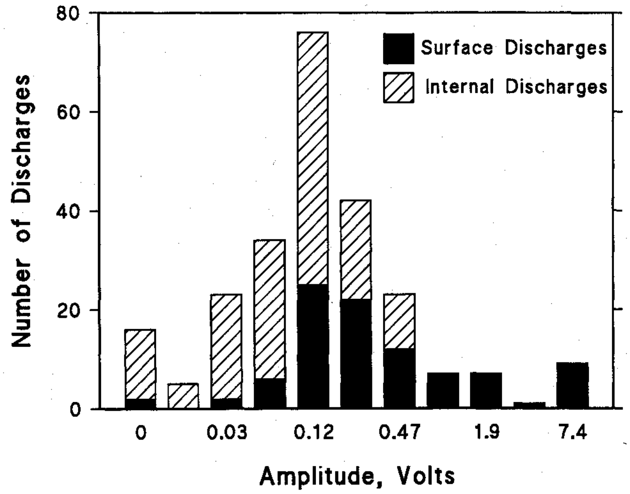

Fig. 1 Amplitude distribution of pulses due to surface and internal discharges.

The SSPMs measure the voltage between the surface of selected materials such as Kapton, Teflon, and quartz fabric and the ground frame of the spacecraft. The spacecraft contains three SSPMs, two on the cylindrical side of the vehicle and one on top. Those on the side of the vehicle move into and out of sunlight as the vehicle rotates at 1 rpm. The one on top was essentially always shadowed by the vehicle. All three contain Kapton samples and the one on top also contains a quartz fabric sample. The Kapton and the quartz fabric samples are used in the study reported here to determine if the surface of the vehicle is charged.

The energetic ion composition experiment measures 100-eV–32-keV ions. The instrument also includes four broadband electron channels from 0.07 to 24 keV.[10,11] The high energy particle spectrometer has four solid-state detectors to measure the energetic electron and proton distributions. The various particles and energy ranges are measured in command-selectable, time- multiplexed modes. The instrument covers electron energies from 0.05 to 10 MeV and protons from 1 to 200 MeV.[10,11]

Data

Pulse analyzer data from a total of 1527 days between February 1979 and March 1988 have been analyzed. Data were collected continuously for most of that time period. The data analyzed to date represent about 45% of the available data. Essentially the entire first year of data has been analyzed. Following the first year only selected periods have been analyzed. This selection has included time periods of known anomalies on other synchronous satellites and time periods containing geomagnetically disturbed days. This selection process may bias the statistics of discharge occurrence presented in the following.

Table 1 contains a summary of the pulses detected by the pulse analyzer during those 1527 days. Pulses occurring within 1 s of a spacecraft command are attributed to a vehicle or payload response to the command and are identified as a command pulse in Table 1. Pulses have also been detected shortly after the time that the ground station command transmitter ceased sending special signals, called s-tones, to the vehicle. These signals enable the space vehicle command receiver. Those pulses are identified as s-tones in Table 1. The majority of the remaining pulses listed in Table 1 occurred during operations of the electron or ion beam experiments.[15] Only 316 of the 8389 pulses cannot be associated with normal vehicle commands or ion and electron beam operations.

Natural Charging

Many of the pulses that cannot be associated with normal vehicle commands or ion and electron beam operations occurred during periods of natural surface charging, that is, during periods when large potentials were measured between surface samples and the vehicle reference frame by the SSPM. The coincidence of these pulses with time periods when the samples were differentially charged and the absence of vehicle commands or mode changes at the time of these pulses has led us to conclude with high confidence that most of the pulses are due to electrostatic discharges.[12] Similar pulses have also been detected during electron and ion beam operations when the surfaces of the samples are artificially charged.[13] Data from the Kapton and the quartz fabric samples on the SSPMs were used to determine if the surface of the vehicle was charged at the time each of the natural discharges was detected. If the potential between any of these four samples and the vehicle frame exceeded 100 V, we consider the surface to have been charged. Natural discharges that were detected when the surface was charged are defined to be surface discharges. Discharges that were detected when the surface was not charged are defined to be internal discharges. Although the 100 V discrimination level is somewhat arbitrary, the separation into the two classes is generally unambiguous. For almost all instances when the samples were not charged, the potentials of these samples were much <100 V and relatively constant. When the samples were charged, the potentials were much >100 V on at least one of the samples and varying over time periods on the order of 1 min.

SSPM data were not available for 45 (14%) of the 316 pulses identified as real discharges. Because all of the pulses that occurred when the vehicle was charged are identified as surface discharges, the number of surface discharges has possibly been somewhat overestimated.

The amplitude distribution of the pulses from the natural discharges is shown in Fig. 1. The voltage plotted along the x axis is the highest discriminator level exceeded by each pulse. The discriminator levels are spaced by about a factor of 2 in voltage. Generally, we find that the amplitudes of the pulses from the surface discharges are larger than the amplitudes of those from the internal discharges at the pulse analyzer sensors. The pulses arising from surface discharges were also significantly larger than pulses detected from normal operations of the vehicle.

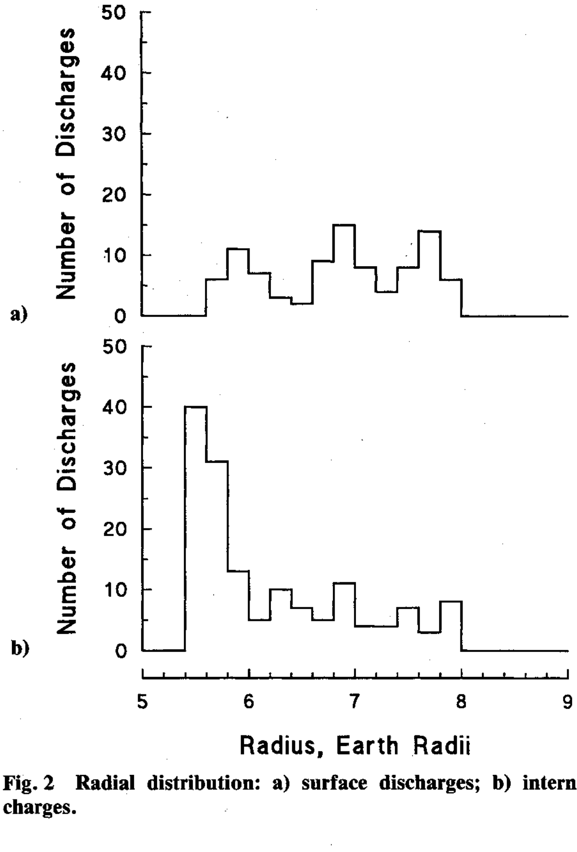

Fig. 2 Radial distribution: a) surface discharges; b) internal discharges.

During a 1-h period on September 22, 1982, 28 pulses were detected while the surface samples on the SSPMs were highly charged. At that time, the planetary magnetic index *Kp* was 8, and the vehicle was located at a radial distance of 5.8 R_e between 0400 and 0500 local time. Because these pulses seriously bias the occurrence statistics, they have been removed from the data reported in this paper. The pulses and vehicle anomalies that occurred on SCATHA on September 22, 1982, have been described by Koons et al.[16]

The occurrence of discharges as a function of the radial distance of the spacecraft from the center of the Earth is shown in Fig. 2. Since the SCATHA satellite has a low inclination (7.5 deg), the radial distance in Fig. 2 is essentially measured in the Earth's equatorial plane. For reference, geosynchronous orbit is at a radial distance of 6.6 R_e. Surface discharges are relatively evenly distributed over the region of space covered by the SCATHA satellite from 5.2 to 7.8 Earth radii. The number of internal discharges increases dramatically at smaller radial distances, with the largest number occurring near the perigee of the SCATHA satellite. The number of internal discharges increases rapidly toward lower altitudes because the maximum intensity of the outer radiation belt is between $L = 4$ and 5, i.e., below the perigee of SCATHA. Thus, the vehicle encounters the more energetic electrons of the outer radiation belt as it approaches perigee.

The occurrence of discharges as a function of the local time at the spacecraft is shown in Fig. 3. Surface discharges peak strongly at midnight and occur in diminishing numbers into the early morning hours. This happens because the electrons responsible for surface charging are injected near geosynchronous orbit near local midnight during a magnetospheric substorm and drift around the morning side of the Earth. Many of the surface discharges at local midnight occurred during the spring and the fall when the spacecraft is eclipsed by the Earth when it is near midnight. Very few surface discharges occurred on the day side of the Earth.

The internal discharges detected on SCATHA occurred preferentially on the day side of the Earth. The maximum in the local-time distribution of internal discharges occurs near noon and thus matches the local-time distribution[17] of relativistic-electron intensities at geosynchronous orbit. At SCATHA's orbit, this asymmetry in local time arises from distortions to the Earth's magnetic field caused by currents on the magnetopause and in the neutral sheet.[18] Because equatorially mirroring electrons drift around the Earth on trajectories of constant B, the day-night asymmetry in the Earth's magnetic field leads to a day-night asymmetry in the geocentric distance to the peak of the outer radiation belt. The peak is at a larger radial distance on the day side than it is at night. Since the spacecraft penetrates farther into the outer radiation belt during the day than it does at night, it experiences higher fluxes of relativistic electrons by day than by night. The flux of 0.5–1-MeV electrons varies by about one order of magnitude from noon to midnight under magnetically quiet conditions.[19]

Discharges are far more likely to occur when the magnetosphere is active, i.e., when the planetary magnetic index *Kp* is 4 or greater. In Fig. 4, the solid curves show the actual number of discharges detected in each category. The dashed curves show the distribution that would have occurred if the discharges were distributed with the same statistical frequency as *Kp*. The distribution of *Kp* for the time period from 1932 through 1986 was used to determine the dashed curves in Fig. 4. A comparison of the histograms shows that both surface and internal discharges are far more likely to occur when the magnetosphere is active, i.e., when *Kp* is >4. Very few surface discharges occur below $Kp = 4$. Those that do were most likely caused by electrons injected by small, local substorms that did not influence the planetary magnetic index *Kp*.

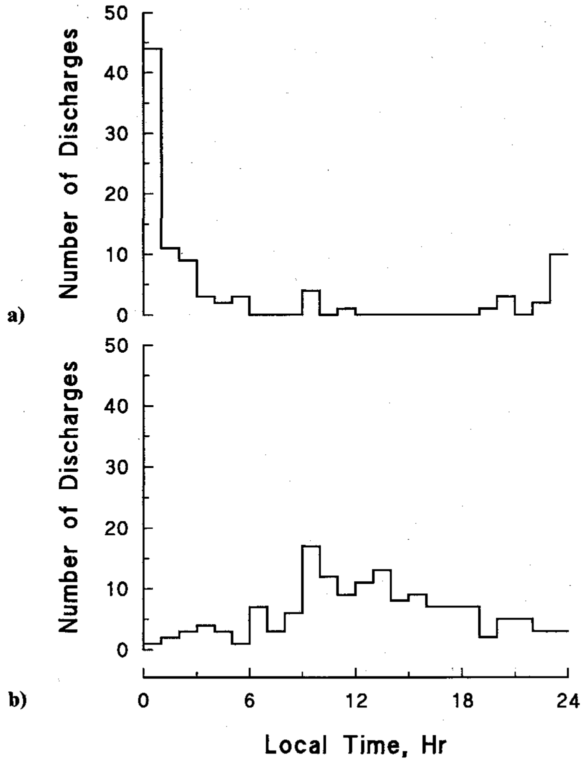

Fig. 3 Local time distribution: a) surface discharges; b) internal discharges.

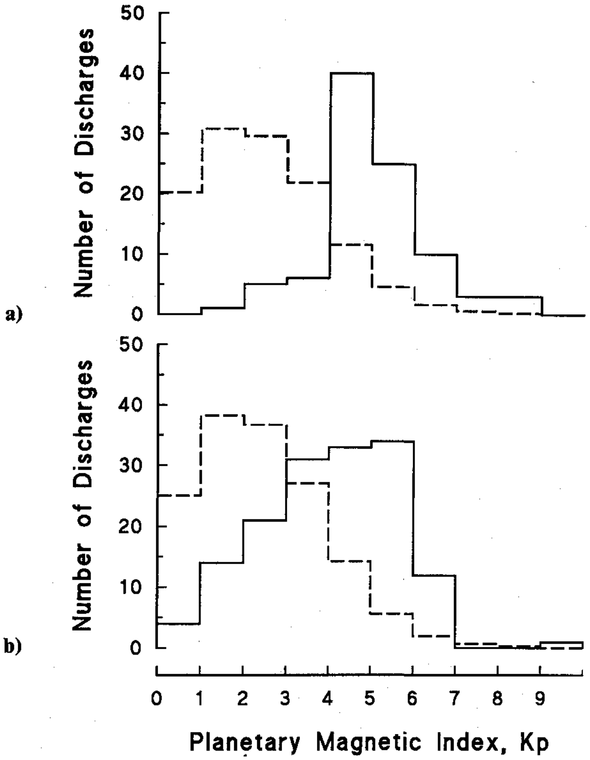

Fig. 4 *Kp* distribution: a) surface discharges; b) internal discharges.

Electron Data

The high energy particle spectrometer[10,11] on SCATHA measures low energy (LE) electrons from 50 to 100 keV, medium energy (ME) electrons from 100 keV to 1 MeV, and high energy (HE) electrons from 1 to 10 MeV. The energetic ion composition experiment[10,11] measures LE electrons from 0.07 to 24 keV. The summary plots of the data from the SSPM which have been produced over the past decade for the time of each discharge on the spacecraft contain time-series graphs of the count rates for electrons from the 0.18, 0.84, 3.9, 18.4, 57,

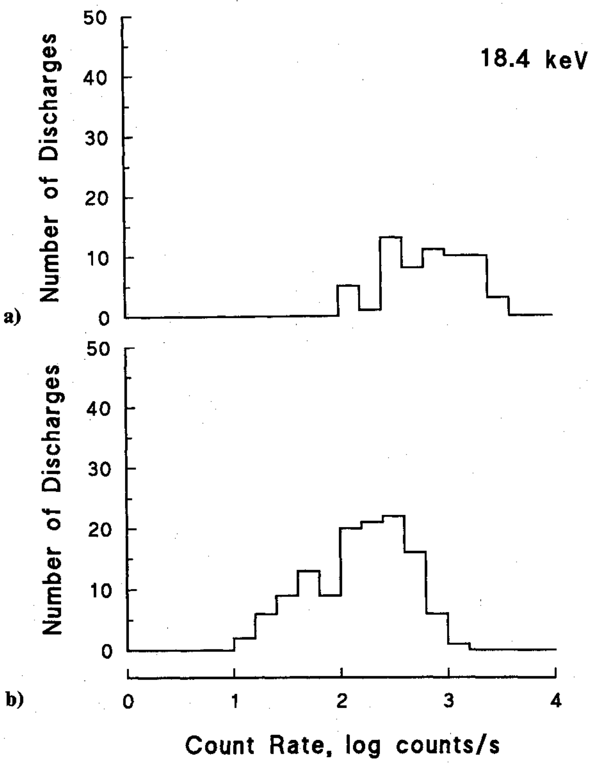

Fig. 5 Distribution of discharges as a function of the count rate of 18.4-keV electrons: a) surface discharges; b) internal discharges.

140, and 288 keV channels from the energetic ion composition experiment and the high energy particle spectrometer. The 18.4- and 288-keV channels will be used here to show the relationship between LE and ME electrons and discharges due to surface and internal charging.

Figure 5 shows the number of discharges detected as a function of the count rate of the 18.4-keV electron channel. The number of surface discharges increases dramatically as the flux of 18.4-keV electrons increases. Surface discharges occur above 100 counts/s and dominate the internal discharges for count rates above 1000 counts/s. Bulk discharges occur at low count rates near the threshold of this channel at 10 counts/s and disappear above a count rate of 1000/s. The flux of ME and HE electrons decreases during the main phase of a geomagnetic storm, whereas the flux of LE electrons increases due to substorm injections of electrons into the inner plasma sheet.[20,21] This is responsible for the decrease in the number of internal discharges at times when the flux of LE electrons is high. The flux of HE electrons then increases as geomagnetic activity returns to quiet levels following the main phase of a magnetic storm.

Figure 6 shows the number of discharges detected as a function of the flux of 288-keV electrons. The number of internal discharges increases dramatically for fluxes above 3600 electrons/(cm^2-s-sr-keV), whereas the number of surface discharges appears for the most part to be unrelated to the flux of 288-keV electrons. Unfortunately, we do not have data from these instruments when discharges were not detected, and so it is not possible to convert the data in Figs. 5 and 6 to probability distributions.

Figure 7 shows a scatter plot of the discharges with the count rate for the 288-keV electrons on the ordinate and the count rate for the 18.4-keV electrons on the abscissa. All of the surface discharges, identified by squares in Fig. 7, occur above an 18.4-keV count rate of 100. Once the count rate exceeds 100, there is little correlation between the count rates for the two energies when surface discharges occur. Most of the internal discharges, identified by a solid circle in Fig. 7, appear in a relatively limited area of the diagram that increases more slowly in the 288-keV count rate than in the 18.4-keV count rate.

High Energy Electron Estimator

It would be useful to spacecraft operators to be able to forecast days on which internal discharges are likely to occur on spacecraft in synchronous orbit. Internal charging of dielectrics is caused by the buildup of charge within the material. It is related to the fluence of ME and HE electrons over a period that is comparable to the decay time of the charge in the dielectric. The decay time depends on the resistivity of the material. This may be very large for a material such as Teflon. Thus, internal discharges are expected to be related to the fluence of ME and HE electrons over a period of hours or

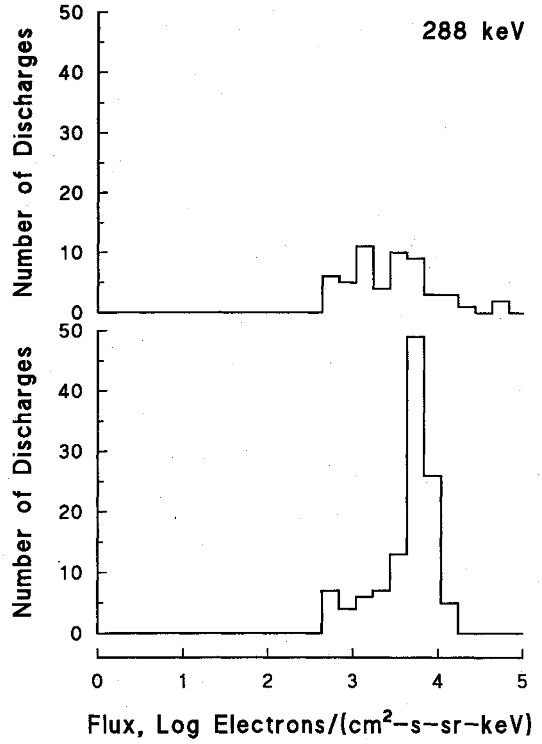

Fig. 6 Distribution of discharges as a function of the flux of 228-keV electrons: a) surface discharges; b) internal discharges.

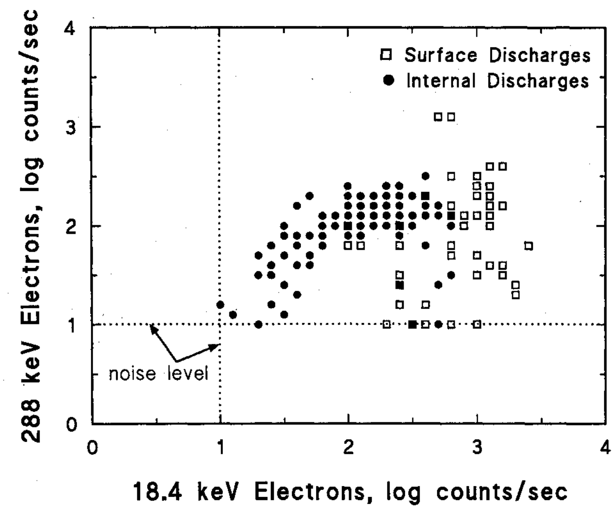

Fig. 7 Scatter plot of discharges as a function of the 18.4- and 228-keV count rates (the solid squares are overlapping hollow squares and solid circles).

even days. We have used two techniques, a linear prediction filter and a neural network model, to estimate the daily fluence of ME and HE electrons on days when SCATHA experienced discharges.

Nagai[21] and Baker et al.[22] used linear prediction filter analysis to predict the relationship between solar wind and geomagnetic indices and the flux of relativistic electrons at synchronous orbit. Nagai[21] showed that the average flux of electrons with energies > 2 MeV at synchronous orbit is well estimated by applying a 20-day linear prediction filter relating the daily ΣKp to the electron flux. The following calculation was used to estimate the daily fluence of electrons with energies > 300 keV from the flux of electrons with energies > 2 MeV obtained from the direct application of Nagai's filter. We assume that the electrons have a spectral shape given by[23]

$$\frac{\mathrm{d}J}{\mathrm{d}E} = \left(\frac{\mathrm{d}J}{\mathrm{d}E}\right)_o \exp\left(\frac{-E}{E_o}\right)(\mathrm{cm}^2/\mathrm{s\text{-}sr\text{-}keV}) \tag{1}$$

with $E_o = 600$ keV. A typical value for $(\mathrm{d}J/\mathrm{d}E)_o$ is 1.3×10^4. The flux above energy E_L is then given by the double integral over solid angle and energy:

$$J = \int_0^{4\pi} \int_{E_L}^{\infty} \left(\frac{\mathrm{d}J}{\mathrm{d}E}\right)_o \exp\left(\frac{-E}{E_o}\right) \mathrm{d}\Omega\, \mathrm{d}E \tag{2}$$

then,

$$J = 4\pi \left(\frac{\mathrm{d}J}{\mathrm{d}E}\right)_o E_o \exp\left(\frac{-E_L}{E_o}\right) \tag{3}$$

To compare the flux above two different energy levels, E_1 and E_2, we can take the ratio $R = J_1/J_2$, which is given by

$$R = \exp[(E_2 - E_1)/E_o] \tag{4}$$

If E_2 is 2 MeV and E_1 is 300 keV, then the ratio for $E_o = 600$ keV is about 17. If the instantaneous integral flux >2 MeV, $J_{(>2\ \mathrm{MeV})}$, is known, then the average daily fluence >300 keV is given by

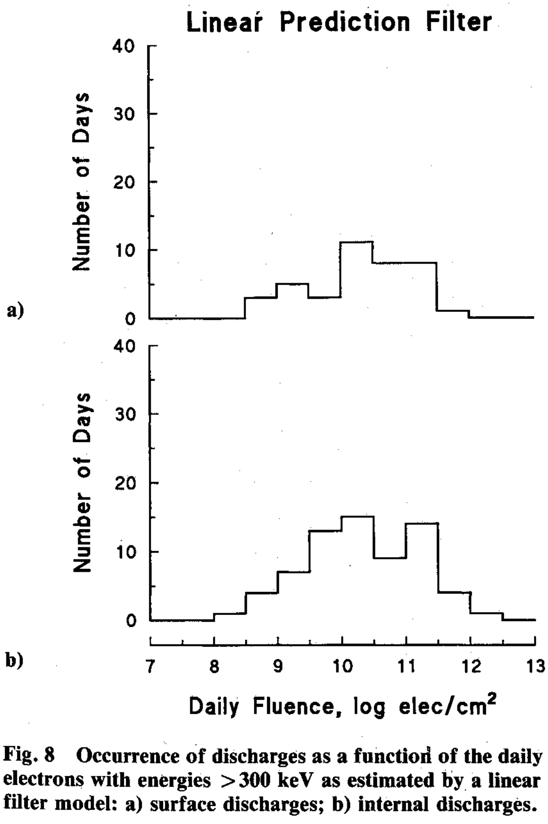

Fig. 8 Occurrence of discharges as a function of the daily fluence of electrons with energies >300 keV as estimated by a linear prediction filter model: a) surface discharges; b) internal discharges.

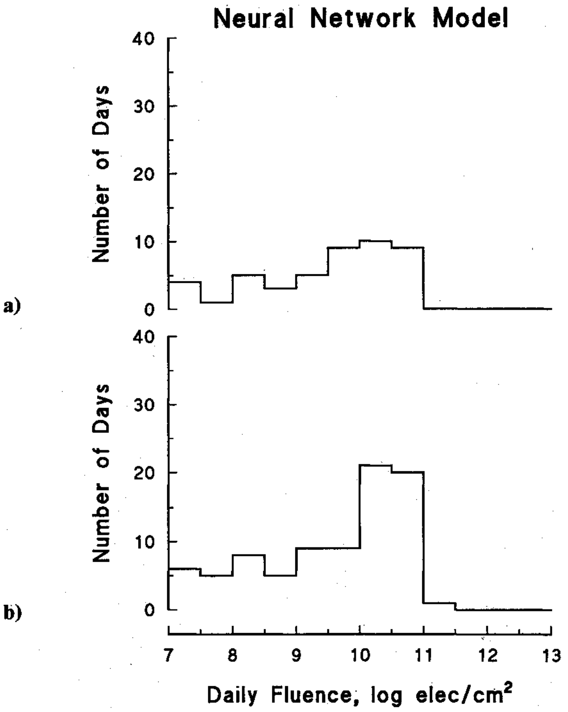

Fig. 9 Occurrence of discharges as a function of the daily fluence of electrons with energies >300 keV as estimated by a neural network model: a) surface discharges; b) internal discharges.

$$F = R_{(300\ \mathrm{keV}/2\ \mathrm{MeV})}\, \mathcal{J}_{(>2\ \mathrm{MeV})}\, \Delta\Omega\, \Delta t \tag{5}$$

where $\mathcal{J}_{(>2\ \mathrm{MeV})}$ is the instantaneous integral flux averaged over a day of electrons with energies >2 MeV. For $\Delta\Omega = 4\pi$ and $\Delta t = 86{,}400$ s, $F = 1.85 \times 10^7\ \mathcal{J}_{(>2\ \mathrm{MeV})}$.

This technique was used to estimate the average daily fluence for each day that a discharge occurred on SCATHA. Figure 8 shows the number of days with discharges as a function of the average daily fluence of electrons with energies >300 keV obtained from the linear prediction filter. The filter derived by Nagai peaks two days before the day of the estimate and is in fact negative for zero time lag. This agrees with the temporal behavior of HE electrons at synchronous orbit.[24]

We have previously developed a neural network to model the temporal behavior of >3-MeV electrons at geosynchronous orbit based on model inputs consisting of 10 consecutive days of the daily sum of the planetary magnetic index ΣKp.[25] The neural network model provides results that are significantly more accurate than those from linear prediction filters. In order to compare the results for the neural network model with those from Nagai's linear prediction filter, we have scaled the daily fluence obtained from the neural network for 3 MeV to 300 keV. The scaling factor R from Eq. (2) is 90. Figure 9 shows the number of days with discharges as a function of the average daily fluence of electrons with energies >300 keV obtained from the neural network model.

From Figs. 8 and 9, it is apparent that surface discharges are not well ordered with respect to the daily fluence of ME (scaled from HE) electrons using either technique. Nor are the internal discharges ordered by the daily fluence obtained from the linear prediction filter. However, there is a sharp increase in the number of days with internal discharges when the neural network model estimates the daily fluence of 300-keV electrons to be $>10^{10}$ cm^{-2} (equivalent to the daily fluence of 3-MeV electrons being $>1.1 \times 10^8$ cm^{-2}). Using a forecasting technique such as that described by Koons and Gorney,[25] the neural network model could be used to forecast days when internal discharges might occur on synchronous spacecraft.

Summary

Pulses detected on SCATHA have been divided into two groups, those from surface discharges, which occurred when the Kapton and quartz fabric test samples on the surface of the vehicle were charged relative to the vehicle frame, and those from internal discharges, which occurred when the test samples on the surface were not charged. The amplitudes of the pulses from the surface discharges tend to be larger than those from the internal charges.

The occurrence of the two types of pulses from the discharges differs in a number of ways. The internal discharges occur much more frequently near the perigee of the SCATHA satellite, whereas the surface discharges occur evenly over the range of altitudes covered from 5.5 to 8 R_e. The surface discharges have a strong peak in their occurrence at local midnight decreasing toward local morning, whereas the internal discharges have a broader maximum centered on the day side of the Earth. Both types tend to occur while the Earth's magnetic field is disturbed. Although few surface discharges occur when *Kp* is <4, a modest number of internal discharges occur under quiet to normal conditions. Surface discharges have a strong tendency to occur when the flux of tens of keV electrons is high, whereas internal discharges occur when the flux of hundreds of keV electrons is high and the flux of tens of keV electrons is low.

The statistics of surface discharges on the SCATHA spacecraft are dominated by the single charging event on September 22, 1982. The largest amplitude discharges and the most serious satellite anomalies occurred during this event while the spacecraft was in sunlight near perigee at 0430 local time.

The data from the SCATHA spacecraft have confirmed all aspects of the spacecraft charging hypotheses first postulated as a cause of satellite anomalies in the mid-1970s. A direct connection has now been verified between the energetic electron environment, the surface and internal charging of the materials on the vehicle, electrostatic discharges, and spacecraft anomalies.

Acknowledgments

This work was supported by the Space Systems Division of the U.S. Air Force under Contract F04701-88-C-0089. The authors thank P. Mizera of the Aerospace Corporation for the data from the SSPMs and J. B. Reagan, R. Sharp, and R. Nightingale of Lockheed for the data from the High Energy Particle Spectrometer and the Energetic Ion Composition Experiment. We also thank R. Klebesadel, D. Baker, and J. B. Blake for the electron data from spacecraft 1982-019 that was used to generate the neural network model. We wish to thank M. Schulz for useful discussions on relativistic electron intensities in the outer radiation belt. The values of *Kp* used in this study were obtained from the National Oceanic and Atmospheric Administration's Environmental Data and Information Service, National Geophysical Data Center.

References

[1] Pike, C. P., and Bunn, M. H., "A Correlation Study Relating Spacecraft Anomalies to Environmental Data," *Spacecraft Charging by Magnetospheric Plasmas,* edited by A. Rosen, Vol. 47, Progress in Astronautics and Aeronautics, AIAA, New York, 1976, pp. 45–60.

[2] McPherson, D. A., and Schober, W. R., "Spacecraft Charging at High Altitude: The SCATHA Satellite," *Spacecraft Charging by Magnetospheric Plasmas,* edited by A. Rosen, Vol. 47, Progress in Astronautics and Aeronautics, AIAA, New York, 1976, pp. 15–30.

[3] Inouye, G. T., "Spacecraft Charging Anomalies on the DSCS-II, Launch 2 Satellites," *Proceedings of the Spacecraft Charging Technology Conferences,* edited by C. P. Pike and R. R. Lovell, Air Force Geophysics Laboratory, AFGL-TR-7-0051, Hanscom, MA, Feb. 1977, pp. 829–852.

[4] DeForest, S. E., "Spacecraft Charging at Synchronous Orbit," *Journal of Geophysical Research,* Vol. 77, No. 4, 1972, pp. 651–659.

[5] Shaw, R. R., Nanevicz, J. E., and Adamo, R. C., "Observations of Electrical Discharges Caused by Differential Satellite Charging," *Spacecraft Charging by Magnetospheric Plasmas,* edited by A. Rosen, Vol. 47, Progress in Astronautics and Aeronautics, AIAA, New York, 1976, pp. 61–76.

[6] Garrett, H. B., "The Charging of Spacecraft Surfaces," *Reviews of Geophysics and Space Physics,* Vol. 19, No. 4, 1981, pp. 577–616.

[7] Vampola, A. L., "Thick Dielectric Charging on High-Altitude Spacecraft," *Journal of Electrostatics,* Vol. 20, No. 1, 1987, pp. 21–30.

[8] Muelenberg, A., Jr., "Evidence for a New Discharge Mechanism for Dielectrics in a Plasma," *Spacecraft Charging by Magnetospheric Plasmas,* edited by A. Rosen, Vol. 47, Progress in Astronautics and Aeronautics, AIAA, New York, 1976, pp. 237–246.

[9] Robinson, P. A., Jr., "Spacecraft Environmental Anomalies Handbook," Air Force Geophysics Laboratory, GL-TR-89-0222, Hanscom, MA, Aug. 1989, pp. 3-1-3-7.

[10] Stevens, J. R., and Vampola, A. L., "Description of the Space Test Program P78-2 Spacecraft and Payloads," The Aerospace Corporation, SAMSO TR-78-24, El Segundo, CA, Oct. 1978.

[11] Fennell, J. F., "Description of P78-2 (SCATHA) Satellite and Experiments," *The IMS Source Book,* edited by C. T. Russell and D. J. Southwood, American Geophysical Union, Washington, DC, 1982, pp. 65–81.

[12] Koons, H. C., Mizera, P. F., Fennell, J. F., and Hall, D. F., "Spacecraft Charging Results from the SCATHA Satellite," *Astronautics and Aeronautics,* Vol. 18, No. 11, 1980, pp. 44–47.

[13] Koons, H. C., "Aspect Dependence and Frequency Spectrum of Electrical Discharges on the P78-2 (SCATHA) Satellite," *Proceedings of the Spacecraft Charging Technology Conference III,* NASA CP 2182, Nov. 1980, pp. 478–492.

[14] Koons, H. C., "Summary of Environmentally Induced Electrical Discharges on the P78-2 (SCATHA) Satellite," *Journal of Spacecraft and Rockets,* Vol. 20, No. 5, 1983, pp. 425–431.

[15] Koons, H. C., and Cohen, H. A., "Plasma Waves and Electrical Discharges Stimulated by Beam Operations on a High Altitude Satellite," *Artificial Particle Beams in Space Plasma Studies,* edited by B. Grandal, Plenum, New York, 1982, pp. 111–120.

[16] Koons, H. C., Mizera, P. F., Roeder, J. L., and Fennell, J. F., "Severe Spacecraft-Charging Event on SCATHA in September 1982," *Journal of Spacecraft and Rockets,* Vol. 25, No. 3, 1988, pp. 239–243.

[17] Lanzerotti, L. J., Roberts, C. S., and Brown, W. L., "Temporal Variations in the Electron Flux at Synchronous Altitudes," *Journal of Geophysical Research,* Vol. 72, No. 23, 1967, pp. 5893–5902.

[18] Williams, D. J., and Mead, G. D., "Nightside Magnetospheric Configuration as Obtained from Trapped Electrons at 1100 Kilometers," *Journal of Geophysical Research,* Vol. 70, No. 13, 1965, pp. 3017–3029.

[19] Pfitzer, K. A., Lezniak, T. W., and Winckler, J. R., "Experimental Verification of Drift-Shell Splitting in the Distorted Magnetosphere," *Journal of Geophysical Research,* Vol. 74, No. 19, 1969, pp. 4687–4693.

[20] Baker, D. N., Blake, J. B., Klebesadel, R. W., and Higbie, P. R., "Highly Relativistic Electrons in the Earth's Outer Magnetosphere, I. Lifetimes and Temporal History 1979–1984," *Journal of Geophysical Research,* Vol. 91, No. A4, 1986, pp. 4265–4276.

[21] Nagai, Tsugunobu, "Space Weather Forecast: Prediction of Relativistic Electron Intensity at Synchronous Orbit," *Geophysical Research Letters,* Vol. 15, No. 5, 1988, pp. 425–428.

[22] Baker, D. N., McPherron, R. L., Cayton, T. E., and Klebesadel, R. W., "Linear Prediction Filter Analysis of Relativistic Electron Properties at 6.6 R_E," *Journal of Geophysical Research,* Vol. 95, No. A9, 1990, pp. 15,133–15,140.

[23] Baker, D. N., Blake, J. B., Gorney, D. J., Higbie, P. R., Klebesadel, R. W., and King, J. H., "Highly Relativistic Magnetospheric Electrons: A Role in Coupling to the Middle Atmosphere?" *Geophysical Research Letters,* Vol. 14, No. 10, 1987, pp. 1027–1030.

[24] Paulikas, G. A., and Blake, J. B., "Modulation of Trapped Energetic Electrons at 6.6 *Re* by the Direction of the Interplanetary Magnetic Field," *Geophysical Research Letters,* Vol. 3, No. 5, 1976, pp. 277–283.

[25] Koons, H. C., and Gorney, D. J., "A Neural Network Model of the Relativistic Electron Flux at Geosynchronous Orbit," *Journal of Geophysical Research,* Vol. 96, No. A4, 1991, pp. 5549–5556.

Antoni K. Jakubowski
Associate Editor